

ORIGINAL RESEARCH

# Periadventitial Delivery of Simvastatin-Loaded Microparticles Attenuate Venous Neointimal Hyperplasia Associated With Arteriovenous Fistula

Chenglei Zhao, MD; Sean T. Zuckerman, PhD; Chuanqi Cai, MD; Sreenivasulu Kilari, PhD; Avishek Singh, PhD; Michael Simeon, BS; Horst A. von Recum, PhD; Julius N. Korley, PhD; Sanjay Misra , MD

**BACKGROUND:** Venous neointimal hyperplasia and venous stenosis (VS) formation can result in a decrease in arteriovenous fistula (AVF) patency in patients with end-stage renal disease. There are limited therapies that prevent VNH/VS. Systemic delivery of simvastatin has been shown to reduce VNH/VS but local delivery may help decrease the side effects associated with statin use. We determined if microparticles (MP) composed of cyclodextrins loaded with simvastatin (MP-SV) could reduce VS/VNH using a murine arteriovenous fistula model with chronic kidney disease.

**METHODS AND RESULTS:** Male C57BL/6J mice underwent nephrectomy to induce chronic kidney disease. Four weeks later, an arteriovenous fistula was placed and animals were randomized to 3 groups: 20  $\mu$ L of PBS or 20  $\mu$ L of PBS with 16.6 mg/mL of either MP or MP-SV. Animals were euthanized 3 days later and the outflow veins were harvested for quantitative reverse transcriptase–polymerase chain reaction analysis and 28 days later for immunohistochemical staining with morphometric analysis. Doppler ultrasound was performed weekly. Gene expression of vascular endothelial growth factor-A (*Vegf-A*), matrix metalloproteinase-9 (*Mmp-9*), transforming growth factor beta 1 (*Tgf- $\beta$ 1*), and monocyte chemoattractant protein-1 (*Mcp-1*) were significantly decreased in MP-SV treated vessels compared with controls. There was a significant decrease in the neointimal area, cell proliferation, inflammation, and fibrosis, with an increase in apoptosis and peak velocity in MP-SV treated outflow veins. MP-SV treated fibroblasts when exposed to hypoxic injury had decreased gene expression of *Vegf-A* and *Mmp-9*.

**CONCLUSIONS:** In experimental arteriovenous fistulas, periadventitial delivery of MP-SV decreased gene expression of *Vegf-A*, *Mmp-9*, *Tgf- $\beta$ 1* and *Mcp-1*, VNH/VS, inflammation, and fibrosis.

**Key Words:** arteriovenous fistula ■ drug delivery ■ vascular remodeling

Worldwide, more than 2 million patients have end-stage renal disease and the majority require hemodialysis to sustain life. The autologous arteriovenous fistula (AVF) is the preferred hemodialysis vascular access because of the lower risk of complications, decreased need for interventions to maintain patency, and better patency.<sup>1</sup> A durable and reliable vascular access is the lifeline of patients with end-stage renal disease. The first AVF was created in

1966;<sup>2</sup> however, the patency of AVF remains 60% at 1 year.<sup>3</sup>

AVF will develop venous stenosis because of venous neointimal hyperplasia (VNH). The mechanisms responsible for VNH formation are not well understood. Several studies indicate that multiple molecular mechanisms work in concert to contribute to VNH formation, including hypoxic injury to the vessel wall at the time of AVF creation leading to increased

Correspondence to: Sanjay Misra, MD, FSIR, FAHA, Department of Radiology, Mayo Clinic, 200 First Street SW, Rochester, MN 5590. E-mail: misra.sanjay@mayo.edu

For Sources of Funding and Disclosures, see page 14.

© 2020 The Authors and Affinity Therapeutics, LLC. Published on behalf of the American Heart Association, Inc., by Wiley. This is an open access article under the terms of the Creative Commons Attribution-NonCommercial License, which permits use, distribution and reproduction in any medium, provided the original work is properly cited and is not used for commercial purposes.

JAHA is available at: [www.ahajournals.org/journal/jaha](http://www.ahajournals.org/journal/jaha)

## CLINICAL PERSPECTIVE

### What Is New?

- In experimental animal models of hemodialysis arteriovenous fistulas, microparticles loaded with statins delivered to the periadventitia of the outflow vein reduce venous stenosis formation.

### What Are the Clinical Implications?

- These observations provide a rationale for local drug delivery of microparticles loaded with statins for reducing venous stenosis formation associated with arteriovenous fistula.

## Nonstandard Abbreviations and Acronyms

<b>α-SMA</b>	α-smooth muscle actin
<b>AVF</b>	arteriovenous fistula
<b>CD68</b>	cluster of differentiation 68
<b>CDP</b>	cyclodextrin polymer
<b>FSP-1</b>	fibroblast-specific protein-1
<b>HIF-1α</b>	hypoxia-inducible factor-1α
<b>MCP-1</b>	monocyte chemoattractant protein-1
<b>MMP-9</b>	matrix metalloproteinase-9
<b>MP</b>	microparticles
<b>MP-SV</b>	microparticles composed of cyclodextrins loaded with simvastatin
<b>MYH11</b>	myosin heavy chain 11
<b>pSMAD3</b>	phosphorylated mothers against decapentaplegic homolog 3
<b>SV</b>	simvastatin
<b>TGF-β1</b>	transforming growth factor beta 1
<b>TUNEL</b>	terminal deoxynucleotidyl transferase-mediated biotin-deoxyuridine triphosphate nick-end labeling
<b>VNH</b>	venous neointimal hyperplasia

matrix deposition, proliferation and migration of fibroblasts and vascular smooth muscle cells, and inflammation.<sup>4–6</sup> Several genes have been found to be increased including vascular endothelial growth factor-A (*Vegf-A*) and matrix metalloproteinase-9 (*Mmp-9*).<sup>4,7</sup>

Statins are 3-hydroxy-3-methylglutaryl coenzyme A reductase inhibitors that are widely prescribed as cholesterol-lowering agents<sup>8</sup> that also possess anti-inflammatory properties.<sup>9</sup> SV has been shown to reduce gene expression of *Vegf-A* and *Mmp-9*<sup>10</sup> and thereby inhibit VNH by reducing vascular smooth muscle cell migration and proliferation in experimental animal models of vein bypass grafts.<sup>11–13</sup> Systemic

delivery of SV in a murine model of chronic kidney disease with AVF has been shown to have beneficial effects with a decrease in VNH formation and improved vascular remodeling.<sup>10,14</sup> Clinical studies suggest that statins might improve AVF patency,<sup>15,16</sup> and a recent clinical study demonstrated that high-dose statin use is associated with lower risk of AVF failure.<sup>15</sup> However, statin intolerance occurs in many patients, which can present as muscle pain and changes in liver function.

Periadventitial drug delivery can be performed using biodegradable wraps, gels, and particles to prevent VNH/venous stenosis formation because a high dose of drug therapy can be delivered.<sup>17–20</sup> Microparticles (MP) composed of cyclodextrin have been used for drug delivery because of their reliable and durable drug release properties. They have been used to treat cancer,<sup>21</sup> fungal infection, and cardiac disease.<sup>22,23</sup> In the present paper, we tested the hypothesis that periadventitial delivery of MP composed of cyclodextrin loaded with SV (MP-SV) delivered to the periadventitia of the outflow vein of AVF would reduce VNH/venous stenosis formation by decreasing *Vegf-A* and *Mmp-9* gene expression in a murine model of chronic kidney disease with AVF.<sup>4,10</sup> We determined both gene and protein expression changes as well as histomorphometric and immunohistochemical analysis along with ultrasound evaluation after periadventitial delivery of cyclodextrin-loaded SV.

## METHODS

The data that support the findings of this study are available from the corresponding author on reasonable request.

### Cyclodextrin Polymer MP Synthesis

Detailed synthesis of cyclodextrin polymer (CDP) has been previously published.<sup>24</sup> Briefly, lightly cross-linked CD prepolymer was dissolved in water and cross-linked in a single water-in-oil emulsion system using a base-catalyzed epoxide ring opening. Particles were washed extensively with hexanes, acetone, and water to remove any remaining mineral oil and unreacted reagents were then lyophilized before drug loading.

### SV Loading and In Vitro Release of SV From CDP

SV was dissolved in dimethylformamide at 5 mg/mL. CDP MP were placed in the SV-loading solution on a rotisserie shaker for 3 days at room temperature. The MP were spun down at 1000 relative centrifugal force

**Table 1. Primer Sequences Used for RT-PCR Gene Expression Analysis**

Gene	Forward	Reverse
<i>Tbp-1</i>	AAGGGAGAATCATGGACCAG	CCGTAAGGCATCATTGGACT
<i>Tgf-β1</i>	CCTGAGTGGCTGTCTTTTGA	TCGTGGAGTTTGTATCTTTGCTG
<i>Vegf-A</i>	Qiagen confidential	Qiagen confidential
<i>Mmp-9</i>	TGCCTGTGTACACCCACATT	TACAGGGCCCCTTCCTTACT
<i>Mcp-1</i>	GGAGAGCTACAAGAGGATCAC	TGATCTCATTGGTTCCGATCC

*Mcp-1* indicates monocyte chemoattractant protein-1; *Mmp-9*, matrix metalloproteinase-9; RT-PCR, reverse transcriptase–polymerase chain reaction; *Tbp-1*, TATA-binding protein-1; *Tgf-β1*, transforming growth factor beta 1; and *Vegf-A*, vascular endothelial growth factor-A.

and the loading solution removed, washed twice with cold dimethylformamide/water (50/50) to remove any unbound SV, and finally washed again with cold deionized water before freezing and lyophilization.

For in vitro release, MP-SV were weighed, placed into low retention tubes, resuspended in 37°C 1X PBS with 0.2% sodium dodecyl sulfate, and placed on a rotisserie shaker. At 1, 2, 4, 8, and 24 hours and every 24 hours thereafter, MP were centrifuged at 1000 relative centrifugal force, the entire volume of PBS removed, and fresh PBS with 0.2% sodium dodecyl sulfate replaced to model infinite sink conditions. Aliquots were frozen at –80°C until analysis by UV-Vis spectrophotometry was performed at 238 nm. To quantify drug loading, MP-SV were placed into 200-proof ethanol on a rotisserie shaker and SV leached into excess ethanol with frequent solvent changes. SV was quantified by UV-Vis as for release samples.

### In Vitro SV Assay

NIH3T3 fibroblasts (ATCC CRL 1658) were serum starved overnight; 50 000 cells per 2-cm well were incubated in Dulbecco's Modified Eagle Medium (containing 10% fetal bovine serum, 100 U/mL penicillin, and 100 U/mL streptomycin) in a cell culture incubator. For the SV dose experiment, cells were treated with

both 1 and 10 μmol/L of SV from α-MP, after 8 hours of incubation in normoxia and hypoxia chamber as previously described.<sup>25</sup> RNA was isolated for gene expression as previously described.<sup>26,27</sup> Experiments were performed in triplicate.

### Animal Models

We obtained approval from the Mayo Clinic Institutional Animal Care and Use Committee before performing any experiments. Male C57BL/6J mice (6–8 weeks old, Jackson Labs, Bar Harbor, ME) were used. They were housed in an animal facility with a 12-hour light/dark cycle, 21°C, and access to food and water ad libitum. Before all procedures, ketamine (120 mg/kg) and xylazine (10 mg/kg) were used to induce anesthesia, which was then maintained by using ketamine (40 mg/kg) and xylazine (3 mg/kg) with intraperitoneal injection. Each mouse underwent partial nephrectomy and AVF creation. At day –28, chronic kidney disease was created by surgical removal of the right kidney, accompanied with ligation of the upper polar artery of the left kidney. Four weeks later, an AVF was created by connecting the end of the left carotid artery to the end of the right jugular vein using a 24-gauge cuff (Patterson Veterinary, Greeley, CO). During the AVF creation, carotid artery and outflow vein were flushed

**Table 2. Antibodies Used for Immunostaining**

Antibody	Host	Catalog Number	Source	Concentration
α-SMA	Rabbit	ab5694	Abcam	1:1000
MYH11	Rabbit	ab53219	Abcam	1:1000
FSP-1	Rabbit	07-2274	EMD Millipore	1:1000
Hif-1α	Rabbit	ab2185	Abcam	1:800
VEGF-A	Rabbit	ab46154	Abcam	1:900
MMP-9	Rabbit	ab38898	Abcam	1:1500
Ki-67	Rabbit	ab9260	EMD Millipore	1:400
pSMAD3	Rabbit	ab52903	Abcam	1:100
MCP-1	Rabbit	ab25124	Abcam	1:1000
CD68	Rabbit	ab125212	Abcam	1:1000

α-SMA indicates α-smooth muscle actin; CD68, cluster of differentiation 68; FSP-1, fibroblast-specific protein-1; MCP-1, monocyte chemoattractant protein-1; MMP-9, matrix metalloproteinase-9; MYH11, myosin heavy chain 11; pSMAD3, phosphorylated mothers against decapentaplegic homolog 3; and VEGF-A, vascular endothelial growth factor.

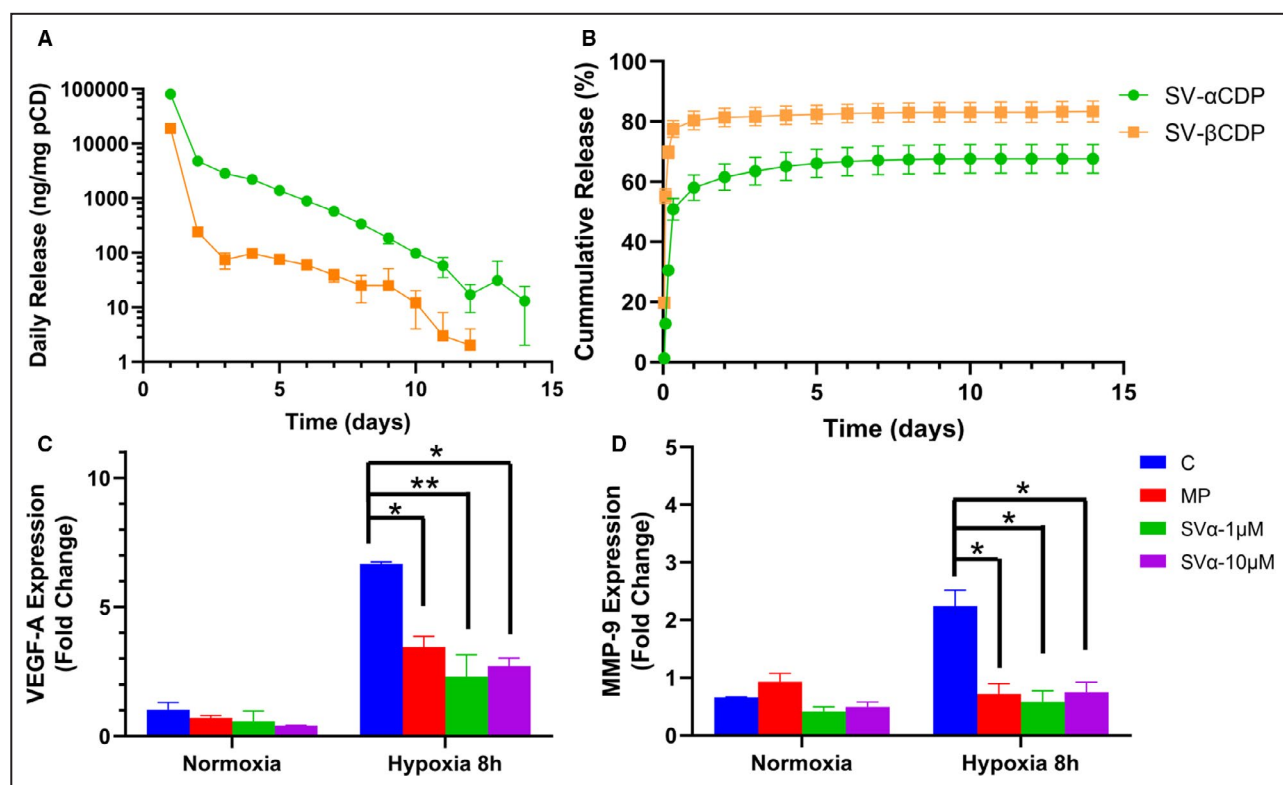


**Figure 1. MP characterization and in vitro inhibition of *Vegf-A* and *Mmp-9* gene expression.**

**A**, There was an increase in SV release from SV- $\alpha$ CDP compared with SV- $\beta$ CDP from day 1 to day 14. **B**, There was an initial burst in both MP, starting from day 1 to day 4. **C** and **D**, There is a significant decrease in *Vegf-A* and *Mmp-9* gene expression in NIH3T3 cells treated with 1  $\mu$ mol/L SV- $\alpha$ -MP and 10  $\mu$ mol/L SV- $\alpha$ -MP concentration of SV subjected to 8 hours of hypoxia compared with control and MP groups. Analysis of variance with repeated measures with post hoc Bonferroni's correction was performed in (**C** and **D**). Each bar represents mean $\pm$ SD of 3 independent experiments. Significant differences are indicated by \* $P$ <0.05 or \*\* $P$ <0.01. C indicates controls; CDP, cyclodextrin polymer; MMP-9, matrix metalloproteinase-9; MP, microparticles; pCD, polymerized cyclodextrin; SV, simvastatin; and VEGF-A, vascular endothelial growth factor-A.

with heparinized saline. PBS (20- $\mu$ L), MP (20- $\mu$ L of 16.6-mg/mL), and MP-SV (20- $\mu$ L of 16.6-mg/mL) were applied to the periadventitia of the outflow vein just distal to the anastomosis circumferentially for a length of 5 mm at the time of AVF creation. Subcutaneous injection with 0.5 mL of warm saline was administered in all animals and they were kept on a warm plate until full recovery. The mice were euthanized 3 and 28 days after AVF creation.

### Serum Urea Nitrogen, Creatinine, Aspartate Aminotransferase and Alanine Aminotransferase Assay

Blood was removed to determine the serum urea nitrogen and creatinine at the time of nephrectomy, AVF placement, day 14 and 28 after AVF creation. We used the QuantiChrom Urea Assay Kit (BioAssay Systems, Hayward, CA) and mouse creatinine assay kit (Crystal Chem, Elk Grove Village, IL) to determine the serum urea nitrogen and creatinine, respectively. The Preventive Care Profile Plus rotor (Abaxis, Union

City, CA) was used to determine the serum alanine aminotransferase, aspartate aminotransferase, total bilirubin, and albumin using a Vetscan VS2 machine (Abaxis, Union City, CA).

### Doppler Ultrasound

Anesthesia was induced and maintained by intraperitoneal injection of ketamine (10 mg/kg) and xylazine (1 mg/kg). Doppler ultrasound was performed to determine the peak velocity in the outflow vein at 7, 14, 21, and 28 days after AVF creation as described previously.<sup>28–31</sup>

### Tissue Collection and Processing

Mice were euthanized at day 3 and outflow vein and contralateral jugular vein placed in RNA later (QIAGEN, Hilden, Germany) for quantitative reverse transcriptase–polymerase chain reaction analysis. Mice were euthanized at day 28 and the outflow vein was removed and flushed with PBS and placed in 10% formalin (Fisher Scientific, Pittsburgh, PA). Each outflow

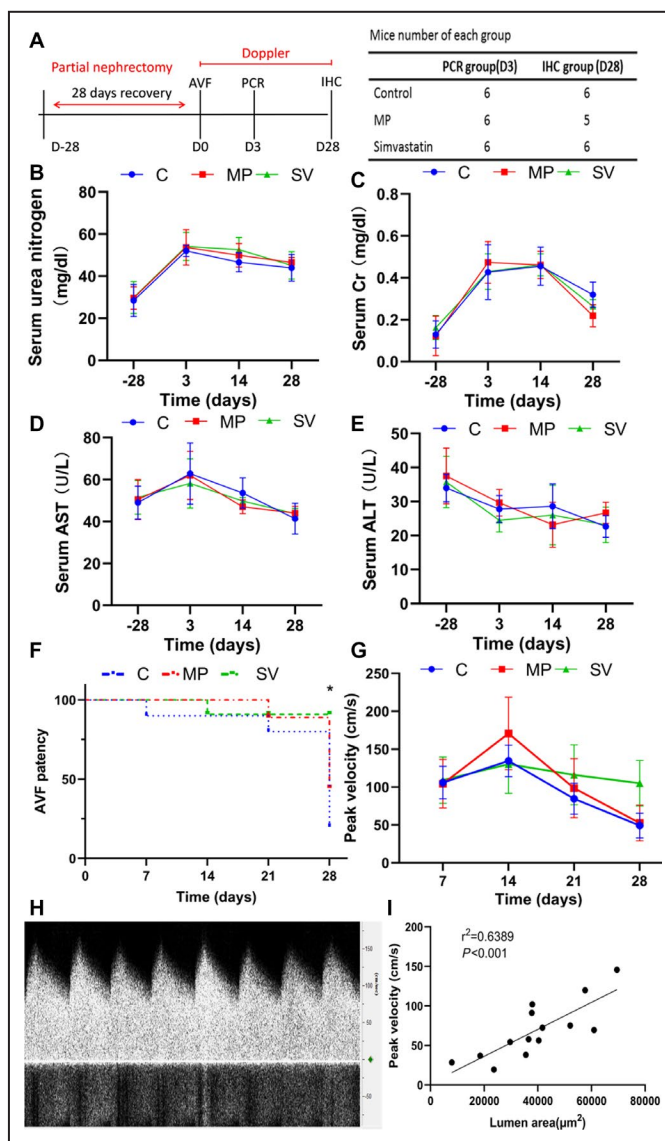


**Figure 2. Murine outcomes after surgery.**

**A**, study design. **B** and **C**, After nephrectomy, all groups had a significant increase in the average serum urea nitrogen and creatinine compared with baselines. No significant difference was observed between each group (C=6, MP=5, SVn=6). **D** and **E**, There was no significant difference between the average ALT and AST levels at any of the time points (C=5, MP=5, SV=6). **F**, At day 28, there was a significant increase in the patency of the outflow veins treated with MP loaded with SV (83%) when compared control (16.7%) and MP (40%,  $P<0.05$ , Figure 2D) (day 7, C=5, MP=5, SV=6; day 14, C N=5, MP N=5, SV N=5; day 21, C N=4, MP N=4, SV N=5; day 28, C N=1, MP N=2, SV N=5). Log rank test was performed. **G**, At day 28, there was a significant increase in the average peak velocity of simvastatin treated vessels compared with C and MP groups (C N=5, MP N=5, SV N=5). **H**, Representative image of the Doppler signal of the outflow vein. **I**, Regression analysis showed a positive correlation between peak velocity and lumen area ( $r^2=0.6389$ ,  $P<0.001$ ). Analysis of variance with repeated measures with post hoc Bonferroni's correction was performed (**B** through **E** and **G**). Each bar represents mean±SD. Significant differences are indicated by \* $P<0.05$ . ALT indicates alanine aminotransferase; AST, aspartate aminotransferase; AVF, arteriovenous fistula; C, controls; Cr, creatinine; IHC, immunohistochemistry; MP, microparticles; PCR, polymerase chain reaction; and SV, simvastatin.

vein was embedded in paraffin lengthwise and cut into 50, 4- $\mu$ m thin contiguous sections and stained with hematoxylin and eosin (H & E), Masson's trichrome (Thermo Fisher Scientific, Waltham, MA), and other stains as outlined subsequently.

### RNA Isolation and Quantitative Reverse Transcriptase–Polymerase Chain Reaction Analysis

Complementary DNA was prepared using the iScript kit (Bio-Rad, Hercules, CA) according to the manufacturer's protocol. Real-time polymerase chain reaction was performed using the iTaq universal SYBR green super mix (Bio-Rad) in a C1000 thermal cycle equipped with a CFX96 Real Time System, and *cq* values were measured using Bio-Rad CFX Manager software. The  $\Delta$ *cq* values were normalized to TATA-binding protein-1 gene expression and the fold change in outflow vein gene expression normalized to the respective contralateral vein and calculated using the 2<sup>–(ΔΔCT)</sup> method.<sup>28–31</sup> Primers used for the different genes are listed Table 1.

### Immunohistochemistry and Morphometric Analysis

Immunohistochemical staining was performed as described previously.<sup>26</sup> Sections were immersed in citric acid buffer (pH of 6.0) for antigen retrieval. Endogenous peroxidase and protein block were incubated, followed by primary antibody incubation at 4°C overnight. The primary antibodies are shown in Table 2 and negative control staining was performed using an immunoglobulin G corresponding to the primary antibody species. All images were captured using a Carl Zeiss Imager M2 microscope (Carl Zeiss, Oberkochen, Germany) in order to cover the entire section. Vessel area, cell density, and intensity of chromogen staining were analyzed using a ZEN 2 blue edition version 2.0 (Carl Zeiss) as described.<sup>27,31,32</sup> The  $\alpha$ -SMA ( $\alpha$ -smooth muscle actin), FSP-1 (fibroblast-specific protein-1), MYH11 (myosin heavy chain 11), HIF-1 $\alpha$  (hypoxia-inducible factor-1 $\alpha$ ), VEGF-A (vascular endothelial growth factor-A), MMP-9 (matrix metalloproteinase-9), Ki-67, TUNEL (terminal deoxynucleotidyl transferase-mediated biotin–deoxyuridine triphosphate nick-end labeling), pSMAD3 (phosphorylated mothers against decapentaplegic homolog 3), MCP-1 (monocyte chemoattractant protein-1), and CD68 (cluster of differentiation 68) indexes were calculated by counting the number of positive cells divided by the total number of cells multiplied by 100. Lumen area was calculated by square of lumen perimeter divided by 12.56. Cell density was calculated by the cell number divided by the neointimal area multiplied by 10<sup>6</sup>.

### TUNEL Staining

TUNEL assay was performed using a colorimetric kit (TACS<sup>®</sup> 2 TdT DAB in situ Apoptosis Detection Kit, Trevigen Inc., Gaithersburg, MD) on paraffin-embedded sections from PBS, MP, and SV-treated outflow veins. A negative control was performed with TdT enzyme omitted.<sup>27,31</sup>

### Statistical Analysis

Data are presented as mean $\pm$ SD. All data were analyzed using GraphPad Prism 8 software (GraphPad Software, La Jolla, CA). Analysis of variance with repeated measures followed by a post hoc Bonferroni's correction or a student 2-sample *t* test was used. Log-rank test was performed to assess differences in patency between the groups. For all comparisons, a *P* value of <0.05 was considered statistically significant and denoted by \* (*P*<0.05), \*\* (*P*<0.01), and NS (not significant).

## RESULTS

### MP Characterization

We analyzed drug release from 2 different MP to determine which one to use. MP release studies demonstrated an initial burst of SV from both  $\alpha$ - and  $\beta$ -MP followed by decreasing amounts of SV release through day 14 and 12, respectively (Figure 1A and 1B).  $\alpha$ -MP released more cumulative SV with less initial burst and did so in a more consistent manner over time compared with  $\beta$ -MP (Figure 1B). Based on the release studies, we chose  $\alpha$ -MP.

### $\alpha$ -MP Loaded With SV Decrease Gene Expression of *Vegf-A* and *Mmp-9* in Hypoxic Fibroblasts

We performed in vitro experiments in NIH3T3 cells subjected to hypoxia for 8 hours to determine the dose of SV- $\alpha$ -MP to be used. We determined the gene expression of *Vegf-A* and *Mmp-9* treated with 1  $\mu$ mol/L SV- $\alpha$ -MP (SV $\alpha$ -1  $\mu$ mol/L) and 10  $\mu$ mol/L SV- $\alpha$ -MP (SV $\alpha$ -10  $\mu$ mol/L). We have previously used a similar assay to identify the dose for local drug delivery.<sup>33</sup> There was a significant decrease in the average gene expression of *Vegf-A* in hypoxic fibroblasts treated with SV $\alpha$ -1  $\mu$ mol/L and SV $\alpha$ -10  $\mu$ mol/L (hypoxia: control: 6.66 $\pm$ 0.08, MP: 3.45 $\pm$ 0.42, SV $\alpha$ -1  $\mu$ mol/L: 2.31 $\pm$ 0.84, SV $\alpha$ -10  $\mu$ mol/L: 2.72 $\pm$ 0.30, SV $\alpha$ -1  $\mu$ mol/L versus control average decrease: 65%, *P*<0.01, SV $\alpha$ -10  $\mu$ mol/L versus control; average decrease: 59%, *P*<0.05, MP versus control; average decrease: 48%, *P*<0.05). We also observed a significant decrease in the *Mmp-9* expression in hypoxic fibroblasts treated with SV $\alpha$ -1  $\mu$ mol/L and SV $\alpha$ -10  $\mu$ mol/L (hypoxia:

**Table 3. Serum Total Bilirubin and Albumin Over Time—Serum Total Bilirubin (μmol/L)**

	-28	3	14	28
C	0.325±0.05	0.3±0	0.25±0.08	0.28±0.04
MP	0.3±0	0.28±0.04	0.3±0	0.33±0.08
SV	0.3±0.08	0.28±0.04	0.28±0.04	0.3±0

C indicates control; MP, microparticles; and SV, simvastatin.

control: 2.24±0.48, MP: 0.72±0.31, SVα-1 μmol/L: 0.59±0.26, SVα-10 μmol/L: 0.75±0.29, SVα-1 μmol/L versus control; average decrease: 74%, *P*<0.05, SVα-10 μmol/L versus control; average decrease: 68%, *P*<0.05, MP versus control average decrease: 69%, *P*<0.05 Figure 1C and 1D). Based on these experiments, we chose the lower dose (1 μmol/L) for the in vivo experiments.

### Surgical Outcomes

Thirty-nine male C57BL/6J mice were included in the study. Two mice died after partial nephrectomy, 1 mouse died after AVF creation, and 1 mouse was excluded because of a thickened carotid artery. The study consisted of 35 mice divided into a control group (N=12), MP group (N=11), and SV group (N=12) (Figure 2A). After partial nephrectomy, there was a significant increase in the average serum urea nitrogen and creatinine when compared with baseline and there was no significant difference between the 3 groups (Figure 2B and 2C). Serum aspartate aminotransferase and alanine aminotransferase test results were in the normal range and showed no difference between the 3 groups (Figure 2D and 2E) as did the serum albumin and total bilirubin (Tables 3 and 4).

### Outflow Veins Treated With Periadventitial Delivery of MP-SV Have Increased Average Peak Velocity

At day 28, there was a significant increase in the patency of the outflow veins treated with MP-SV (83%) when compared control (16.7%) and MP (40%, Log-rank: *P*<0.05, Figure 2F). At day 28 after AVF placement, the average peak velocity in SV-treated outflow veins had increased significantly compared with the

**Table 4. Serum Total Bilirubin and Albumin Over Time—Serum Albumin (g/dL)**

	-28	3	14	28
C	3.98±0.1	3.83±0.41	4.24±0.18	3.93±0.23
MP	4.23±0.15	3.82±0.34	4±0.29	4.12±0.16
SV	4.03±0.64	3.93±0.19	3.98±0.16	4.16±0.29

C indicates control; MP, microparticles; and SV, simvastatin.

control and MP vessels (control: 49.21±7.30 cm/s, MP: 52.70±10.56 cm/s, SV: 105.06±29.97 cm/s, SV versus control; average increase: 214%, *P*<0.05, SV versus MP; average increase: 199%, *P*<0.05, Figure 2G).

### Outflow Veins Treated With Periadventitial Delivery of MP-SV Have Decreased Gene Expression of *Vegf-A*, *Mmp-9*, *Tgf-β1*, and *Mcp-1* in AVFs

We assessed gene expression of *Vegf-A*, *Mmp-9*, transforming growth factor beta 1 (*Tgf-β1*), and *Mcp-1* in outflow veins using quantitative reverse transcriptase–polymerase chain reaction at day 3 after AVF placement. There was a significant reduction in the average gene expression of *Vegf-A* (control: 3.56±1.59, MP: 2.83±1.39, SV: 0.54±0.70, SV versus control; average decrease: 84%, *P*<0.01, SV versus MP; average decrease: 81%, *P*<0.05, Figure 3A), *Mmp-9* (control: 5.76±2.69, MP: 5.73±2.57, SV: 1.78±0.67, SV versus control average decrease: 69%, *P*<0.05, SV versus MP; average decrease: 69%, *P*<0.05, Figure 3B), *Tgf-β1* (control: 4.39±1.80, MP: 4.71±1.42, SV: 1.37±0.97, SV versus control; average decrease: 69%, *P*<0.05, SV versus MP; average decrease: 71%, *P*<0.01, Figure 3C), and *Mcp-1* (control: 6.00±2.02, MP: 5.43±3.49, SV: 1.25±1.23, SV versus control; average decrease: 79%, *P*<0.05, SV versus MP; average decrease: 77%, *P*<0.05, Figure 3D).

### Outflow Veins Treated With Periadventitial Delivery of MP-SV Have Increased Positive Vascular Remodeling

We assessed vascular remodeling of the outflow vein by analyzing H & E stained outflow vein sections (Figure 3E). Semiquantitative analysis demonstrated that the average lumen area/neointima ratio was significantly increased in SV-treated vessels compared with the control and MP vessels (control: 0.69±0.45, MP: 0.97±0.35, SV: 2.29±1.06, SV versus control; average increase: 332%; *P*<0.05, Figure 3F). There was a significant decrease in the average neointimal area in SV-treated vessels compared with the control and MP vessels (control: 52 910±21 738 μm<sup>2</sup>, MP: 47 316±13 284 μm<sup>2</sup>, SV: 21 669±8636 μm<sup>2</sup>, SV versus control; average decrease: 59%, *P*<0.05, SV versus MP; average decrease: 54%, *P*<0.05, Figure 3G) and neointimal cell density (control: 21 622±1911/mm<sup>2</sup>, MP: 22 402±3448/mm<sup>2</sup>, SV: 15 578±3966/mm<sup>2</sup>, SV versus control; average decrease: 28%, *P*<0.05, SV versus MP; average decrease: 30%, *P*<0.05, Figure 3H) There was no significant decrease in the average media+adventitia area in the SV group compared with the control group (control: 40 719±14 236/

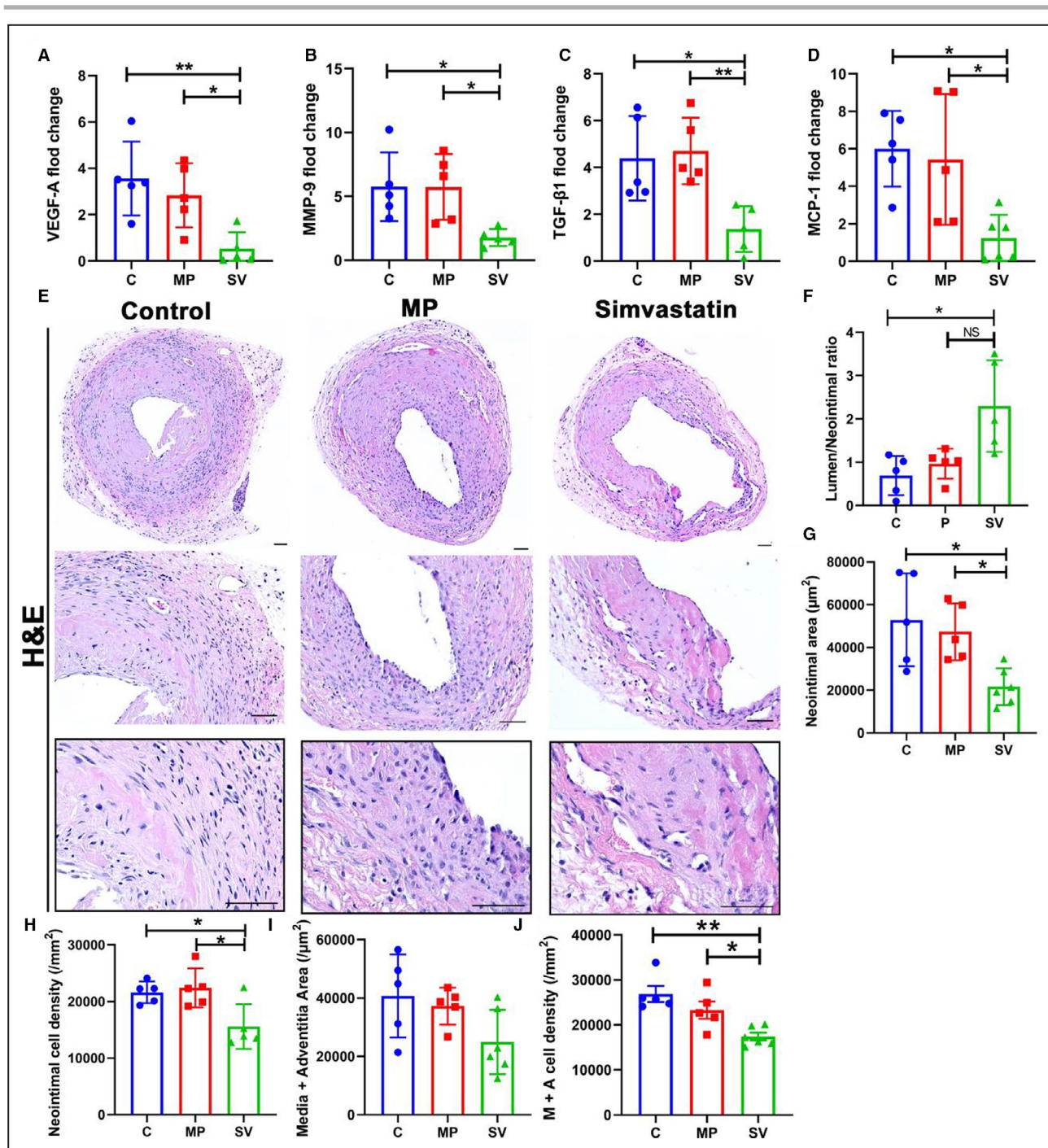
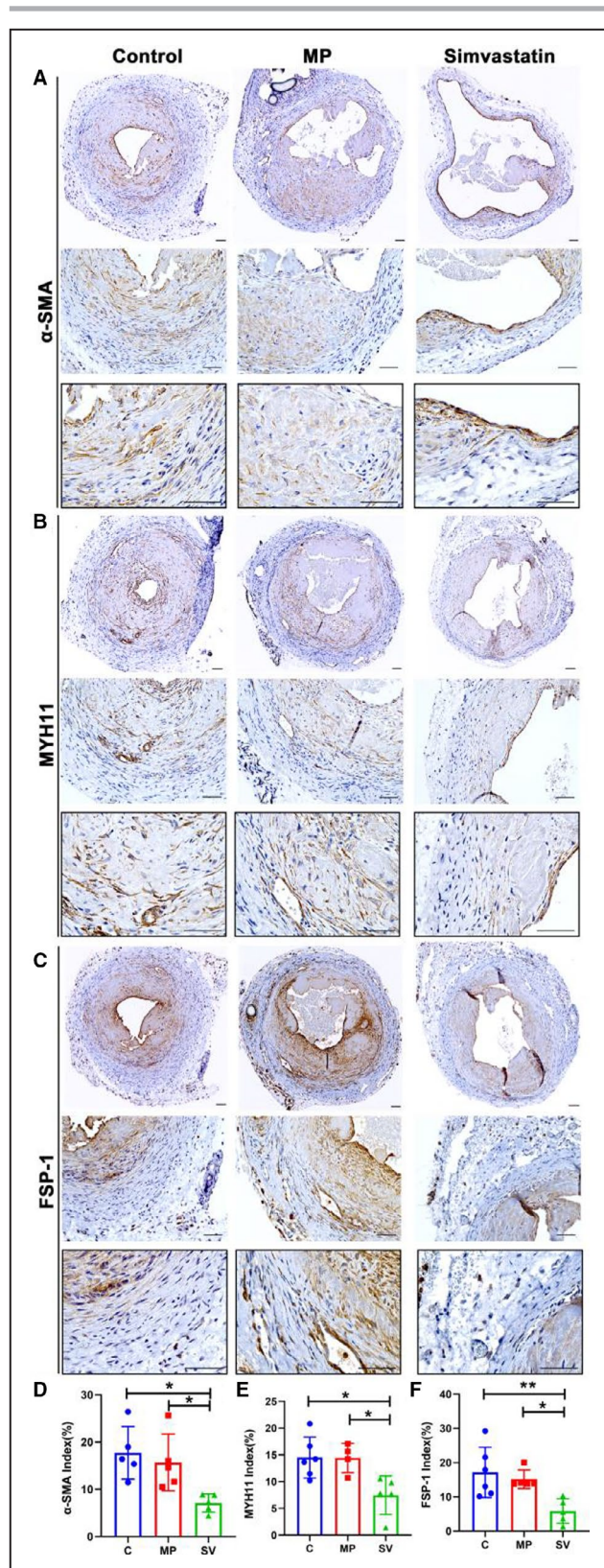


**Figure 3. Decreased gene expression of *Vegf-A*, *Mmp-9*, *Tgf-β1*, and *Mcp-1* increases AVF remodeling in SV group.** A through D, The gene expression of *Vegf-A* (C N=5, MP=5, SV N=5), *Mmp-9* (C N=5, MP N=5, SV N=5), *Tgf-β1* (C N=5, MP N=5, SV N=5), and *Mcp-1* (C N=5, MP N=5, SV N=6) were determined by RT-PCR in AVF outflow vein normalized to the contralateral vein. In SV-treated vessels, there was a significant decrease in the average gene expression of *Vegf-A*, *Mmp-9*, *Tgf-β1*, and *Mcp-1* compared with control and MP group. E, Representative hematoxylin and eosin stained sections for control, MP, and SV-treated outflow veins at day 28, respectively. F, There was a significant increase in the average ratio of the lumen vessel area/neointimal area (C N=5, MP N=5, SV N=5) of SV-treated outflow veins compared with the control group at day 28. G and H, There was a significant reduction in the average neointimal area (C N=5, MP N=5, SV N=6) and neointimal cell density (C N=5, MP N=5, SV N=5) in SV-treated vessels compared with C and MP groups. I and J, There was no significant difference of media+adventitia area (C N=5, MP N=5, SV N=6). A significant decrease in the average media+adventitia cell density (C N=5, MP N=5, SV N=6) was observed in SV-treated vessels compared with control and MP group. Dash line, neointimal area. Two-sample *t* test was performed (A through D and F through J). Each bar represents mean±SD. Significant differences are indicated by \**P*<0.05 and \*\**P*<0.01. NS, not significant. Scale bar is 50 μm. AVF indicates arteriovenous fistula; C, controls; H&E, hematoxylin and eosin; MCP-1, monocyte chemoattractant protein-1; MMP-9, matrix metalloproteinase-9; MP, microparticles; SV, simvastatin; TGF-β1, transforming growth factor beta 1; and VEGF-A, vascular endothelial growth factor-A.



mm<sup>2</sup>, MP: 37 272±6347/mm<sup>2</sup>, SV: 24 962.36±11 025/mm<sup>2</sup>, Figure 3I). The average cell density in the media+adventitia was significantly decreased in the SV-treated vessels compared with the control and MP

**Figure 4. Immunohistochemical staining for α-SMA, MYH11, and FSP-1.**

Representative sections of α-SMA (A), MYH11 (B), and FSP-1 (C) staining at day 28. (D through F) Semiquantitative analysis results showed a significant decrease in the average α-SMA (C N=5, MP N=5, SV N=5), MYH11 (C N=6, MP N=4, SV N=5), and FSP-1 (C N=6, MP N=5, SV N=5) positive index in the SV-treated vessels compared with the C and MP groups at day 28. Cells staining brown are positive for α-SMA, MYH11, and FSP-1. Two-sample *t* test was performed (D through F). Each bar represents mean±SD. Significant differences are indicated by \**P*<0.05 and \*\**P*<0.01. Scale bar is 50 μm. α-SMA indicates α-smooth muscle actin; C, controls; FSP-1, fibroblast-specific protein-1; MP, microparticles; MYH11, myosin heavy chain 11; and SV, simvastatin.

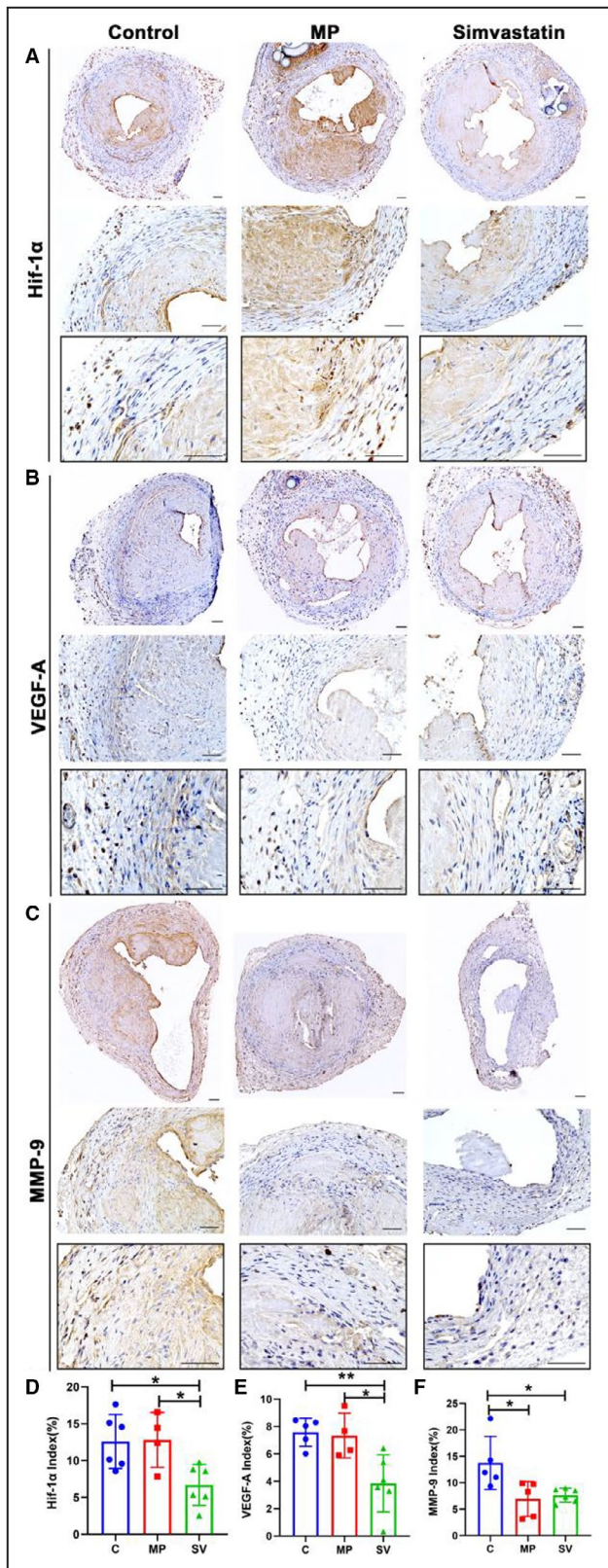
group (control: 26 892±3972/mm<sup>2</sup>, MP: 23 314±4284/mm<sup>2</sup>, SV: 17 427±2093/mm<sup>2</sup>, SV versus control; average decrease: 35%, *P*<0.01, SV versus MP; average decrease: 25%, *P*<0.05, Figure 3J).

### Outflow Veins Treated With Periadventitial Delivery of MP-SV Have Decreased Staining of α-SMA, MYH11, and FSP-1

Immunohistochemical analysis of outflow veins from control animals demonstrated that there were increased α-SMA (+) cells that were localized mainly to the neointima of the outflow veins (Figure 4A). Semiquantitative analysis showed a significant decrease in the average α-SMA index of SV-treated outflow veins compared with the MP and control vessels (control: 17.74±5.56%, MP: 15.69±6.00%, SV: 7.10±1.91%, SV versus control; average decrease: 60%, *P*<0.05, SV versus MP; average decrease: 55%, *P*<0.05, Figure 4D). MYH11 (+) cells were located in the neointima of all groups (Figure 4B). Compared with the control and MP groups, there was a significant decrease in the average MYH11 index in the SV-treated vessels (control: 14.50±3.81%, MP: 14.42±2.75%, SV: 7.46±3.60%, SV versus control; average decrease: 49%, *P*<0.05, SV versus MP; average decrease: 48%, *P*<0.05, Figure 4E). FSP-1 (+) cells were localized in the neointima in the control and MP groups, whereas in the SV group FSP-1 (+) cells were located throughout the vessel (Figure 4C). There was a significant reduction in the average FSP-1 index of SV-treated outflow veins compared with control and MP groups (control: 17.17±7.35%, MP: 15.16±2.72%, SV: 5.86±3.59%, SV versus control; average decrease: 66%, *P*<0.01, SV versus MP; average decrease: 61%, *P*<0.05, Figure 4F).

### Outflow Veins Treated With Periadventitial Delivery of MP-SV Have Decreased HIF-1α, VEGF-A, and MMP-9 Index

To access the extent of hypoxia-induced extracellular matrix deposition, we performed staining of



HIF-1α, VEGF-A, and MMP-9 in the outflow veins at day 28 after AVF creation. HIF-1α (+) cells were present throughout the entire vessel in all groups

**Figure 5. Immunohistochemistry staining for HIF-1α, VEGF-A, and MMP-9.**

**A through C,** Representative stains of HIF-1α (**A**), VEGF-A (**B**) and MMP-9 (**C**) staining at day 28. **D through F,** Semiquantitative analysis showed a significant decrease in the average HIF-1α (C N=6, MP N=4, SV N=6), VEGF-A (C N=5, MP N=4, SV N=6), and MMP-9 (C N=5, MP N=5, SV N=6) index in the SV-treated vessels compared with the control group at day 28. There was also a significant decrease in average HIF-1α and VEGF-A positive index in the SV-treated vessels compared with the MP group. A significant difference was observed in the MP group for average MMP-9 index compared with the control group. Cells staining brown are positive for HIF-1α, VEGF-A, and MMP-9. Two-sample *t* test was performed (**D through F**). Each bar represents mean±SD. Significant differences are indicated by \**P*<0.05 and \*\**P*<0.01. Scale bar is 50 μm. C indicates controls; HIF-1α, hypoxia-inducible factor-1α; MMP-9, matrix metalloproteinase-9; MP, microparticles; SV, simvastatin; and VEGF-A, vascular endothelial growth factor-A.

(Figure 5A). There was a significant decrease in the mean HIF-1α index in the SV-treated outflow veins compared with control and MP groups (control: 12.60±3.66%, MP: 12.81±3.72%, SV: 6.71±2.79%, SV versus control; average decrease: 47%, *P*<0.05, SV versus MP; average decrease: 48%, *P*<0.05, Figure 5D). There was a significant decrease in the average VEGF-A index in the SV-treated vessels compared with the control and MP groups (control: 7.58±1.02%, MP: 7.34±1.63%, SV: 3.33±1.86%, SV versus control; average decrease: 56%, *P*<0.01, SV versus MP; average decrease: 55%, *P*<0.05, Figure 5B and 5E). The average MMP-9 index was significantly decreased in the SV-treated vessels compared with the control and MP groups (control: 14.85±5.05%, MP: 6.94±3.30%, SV: 7.86±1.33%, SV versus control; average decrease: 41%, *P*<0.05, MP versus control; average decrease: 53%, *P*<0.05, Figure 5C and 5F).

### Outflow Veins Treated With Periadventitial Delivery of MP-SV Have Decreased Cell Proliferation and Increased Apoptosis

Ki-67 and TUNEL staining were performed to assess cell proliferation and apoptosis. There was a significant decrease in the average Ki-67 index in the SV-treated vessels compared with the control but not the MP group (control: 39.10±8.58%, MP: 21.57±7.37%, SV: 16.35±9.01%, SV versus control; average decrease: 58%, *P*<0.01, MP versus control; average decrease: 45%, *P*<0.05, Figure 6A and 6C). TUNEL staining was significantly increased in the SV-treated vessels compared with the control and MP groups (control: 9.33±3.29%, MP: 10.54±3.78%, SV: 15.66±2.77%, SV versus control; average increase: 68%, *P*<0.05, SV versus MP; average increase: 49%, *P*<0.05, Figure 6B and 6D).

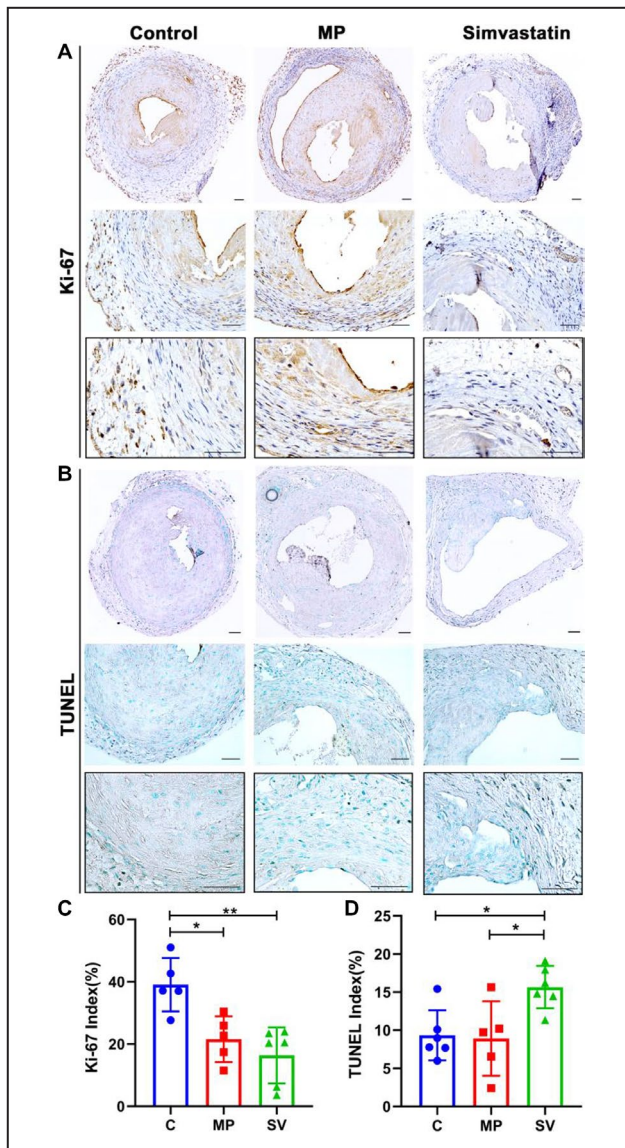


**Figure 6. Immunohistochemistry staining for Ki-67 and TUNEL.** **A**, Representative staining for Ki-67 at day 28. Cells staining brown are positive for Ki-67. **B**, Representative staining for TUNEL. Cells staining black are positive for TUNEL. **C**, Semiquantitative analysis showed a significant decrease in the average Ki-67 positive index in the SV-treated vessels compared with control and MP groups (C N=5, MP N=5, SV N=6). **D**, Semiquantitative analysis showed a significant increase in the average TUNEL positive staining in SV-treated vessels compared with control group and MP group (Control N=6, MP N=5, Simvastatin N=6). Two-sample *t* test was performed (**C** and **D**). Each bar represents mean±SD. Significant differences are indicated by \**P*<0.05 and \*\**P*<0.01. Scale bar is 50 μm. C indicates controls; dUTP, deoxyuridine triphosphate; MP, microparticles; SV, simvastatin; and TUNEL, terminal deoxynucleotid transferase-mediated biotin–deoxyuridine triphosphate nick-end labeling.

### Outflow Veins Treated With Periadventitial Delivery of MP-SV Have Decreased Fibrosis and pSMAD3 Index

Statins have been shown to reduce TGF-β1 expression.<sup>34</sup> TGF-β1 expression was observed to be

significantly increased in AVF creation and failed vascular access both in clinical specimens and experimental animal models.<sup>27,35,36</sup> Vessel fibrosis was assessed using pSMAD3 and Masson’s trichrome staining (Figure 7A and 7B). There was a significant decrease in the pSMAD3 index in the SV-treated vessels compared with control and MP (control: 7.91±3.08%, MP: 7.05±0.99%, SV: 2.60±1.67%, SV versus control; average decrease: 67%, *P*<0.01, SV versus MP; average decrease: 63%, *P*<0.05, Figure 7C). The amount of Masson’s trichrome index was significantly decreased in the SV group compared with the control and MP groups (control: 48.40±10.47%, MP: 46.51±5.11%, SV: 29.94±5.07%, SV versus control; average decrease: 38%, *P*<0.01, SV versus MP average decrease: 36%, *P*<0.05, Figure 7D).

### Periadventitial Delivery of MP-SV Results in Decreased Staining of MCP-1 and CD68

MCP-1 (+) positive cells were located in the media and adventitia layers in all groups (Figure 8A). The mean MCP-1 index was significantly decreased in the SV-treated vessels compared with the control and MP groups (control: 14.90±4.44%, MP: 14.86±6.68%, SV: 6.66±2.50%, SV versus control; average decrease: 55%, *P*<0.05, SV versus MP; average decrease: 55%, *P*<0.05, Figure 8C). CD68 (+) cells were present throughout the whole vessel in the control and MP groups, whereas in SV-treated vessels, most were localized in the media and adventitia layer (Figure 8B). There was a significant decrease in the average CD68 index in the SV-treated vessels compared with the control and MP vessels (control: 15.65±3.06%, MP: 14.19±5.44%, SV: 6.73±3.21%, SV versus control; average decrease: 57%, *P*<0.05, SV versus MP; average decrease: 53%, *P*<0.05, Figure 8D).

## DISCUSSION

In the present study, we demonstrated that periadventitial delivery of MP-SV to the outflow vein of AVF decreases gene expression of *Vegf-A*, *Mmp-9*, *Tgf-β1*, and *Mcp-1* in a murine AVF model. This was accompanied with a reduction in VNH/venous stenosis formation, increased peak velocity, decreased cell density, cell proliferation, inflammation, hypoxia, and an increase in apoptosis. This was accompanied with a reduction in VEGF-A, MMP-9, MCP-1, and pSMAD3 staining. SV-treated NIH3T3 cells when exposed to hypoxia had decreased *Vegf-A* and *Mmp-9* gene expression.

It is hypothesized that VNH occurs in AVF because of multiple etiologies including hypoxic injury after creation of AVF, an increase in inflammation due to the end-stage renal disease milieu, abnormal flow patterns, and shear stress leading to smooth muscle proliferation,

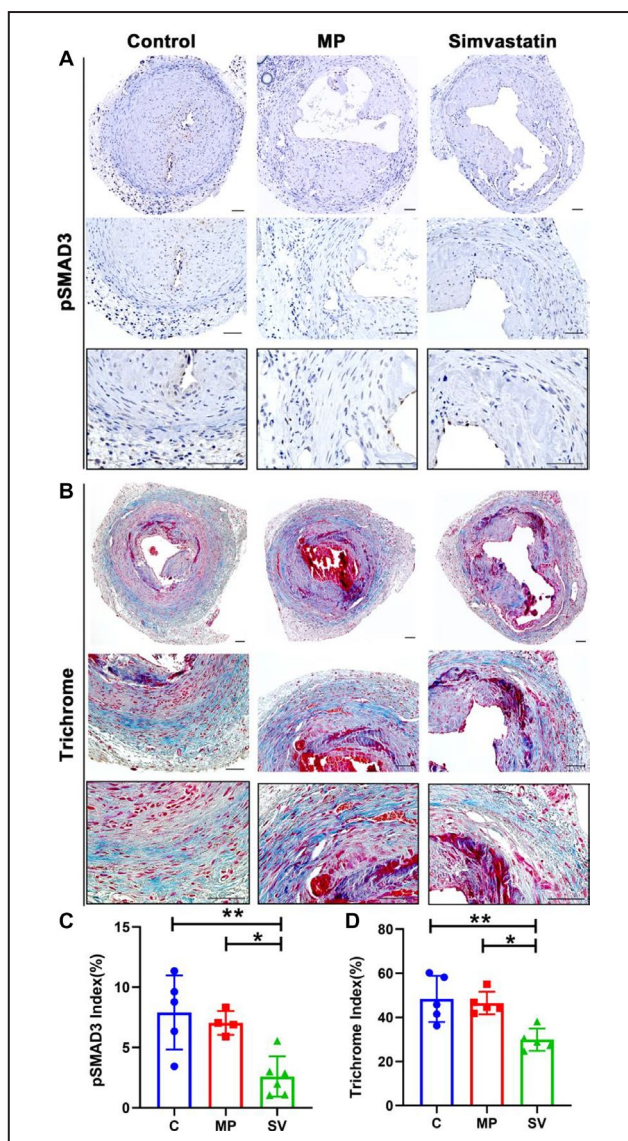


**Figure 7. Immunohistochemistry staining for pSMAD3 and fibrosis.**

There is decreased fibrosis in SV-treated vessels as assessed using Masson's trichrome and pSMAD3 staining. **A** and **B**, Representative staining of pSMAD3 (**A**) and Trichrome (**B**) staining at day 28. **C** and **D**, Semiquantitative analysis showed a significant decrease in the pSMAD3 (C N=5, MP N=4, SV N=6) and the trichrome-positive index (C N=5, MP N=5, SV N=5) in the SV-treated vessels compared with the control and MP group. Cells staining brown are positive for pSMAD3. Two-sample *t* test was performed (**C** and **D**). Each bar represents mean±SD. Significant differences are indicated by \**P*<0.05 and \*\**P*<0.01. Scale bar is 50 μm. C indicates controls; MP, microparticles; pSMAD3, phosphorylated mothers against decapentaplegic homolog 3; and SV, simvastatin.

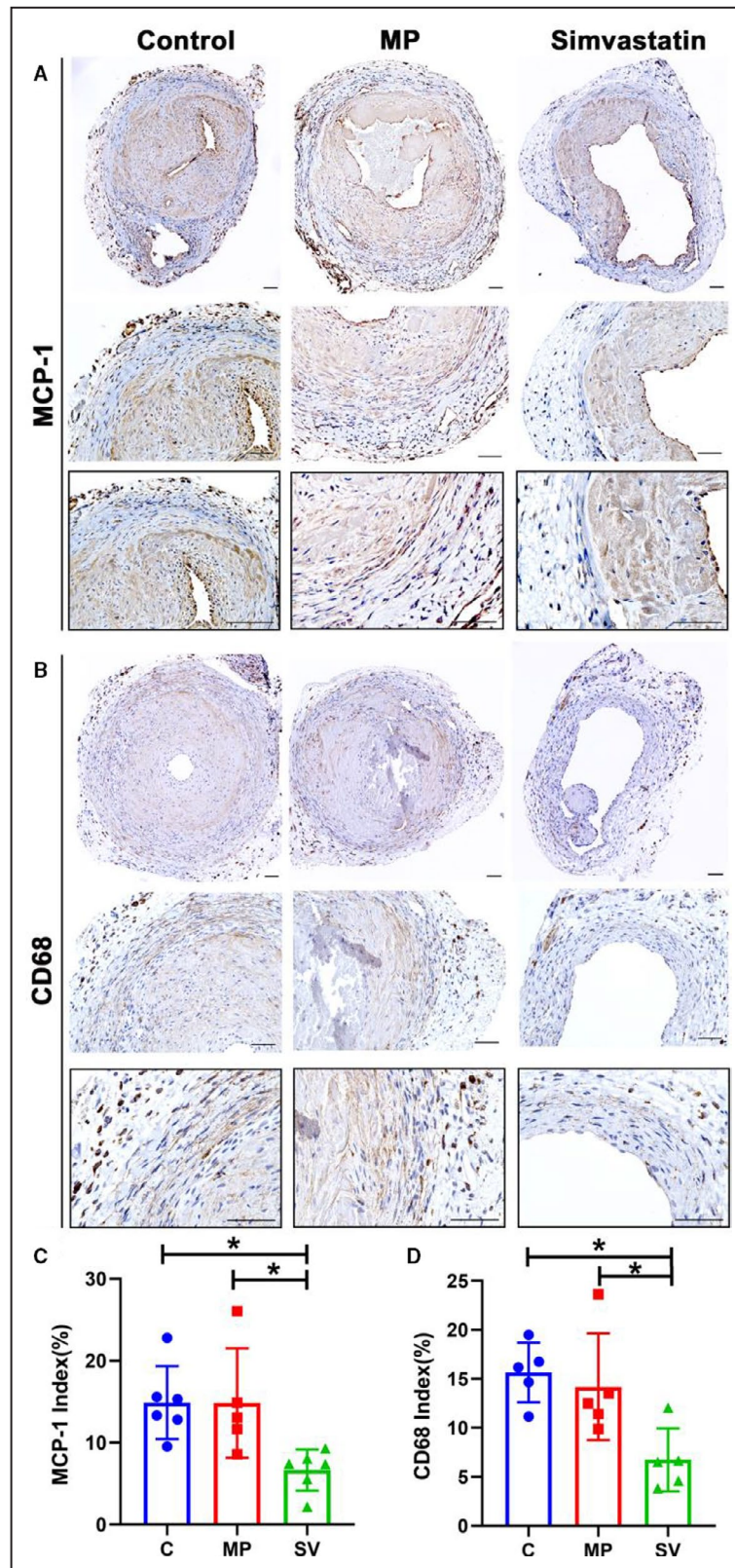
extracellular matrix deposition, and fibrosis causing venous stenosis.<sup>10,37</sup> Studies have demonstrated that there is increased expression of HIF-1α in experimental animal models and clinical samples of failed hemodialysis vascular access specimens.<sup>4,38</sup> The present study demonstrated a reduction in HIF-1α staining in SV-treated vessels compared with controls. Previous studies have demonstrated that hypoxic injury can result in differentiation of fibroblasts to myofibroblasts.<sup>25</sup> Moreover, when NIH3T3 cells were subjected to hypoxia and treated with MP-SV, there was a reduction in *Vegf-A* and *Mmp-9* gene expression. Previous research in experimental animal models has shown that there is increased expression of *Vegf-A* and *Mmp-9* before venous stenosis formation.<sup>4,7</sup> Reducing *Vegf-A* expression using lentiviral techniques decreased VNH with increased lumen vessel area.<sup>39</sup> We hypothesized that locally delivered MP-SV would decrease hypoxia-induced VNH via VEGF-A/MMP-9 signaling. Our results indicated that SV decreased expressions of HIF-1α, VEGF-A, and MMP-9 in periadventitial delivery of day 28 AVF outflow veins. In addition, the average gene expression of *Vegf-A* and *Mmp-9* was reduced and these results are consistent with our previous studies.<sup>10</sup>

In human AVF and experimental animal models, increased TGF-β1 expression has been observed in stenotic segments.<sup>27,35,40</sup> An increase in TGF-β1 can induce vascular fibrosis through pSMAD3 signaling.<sup>40</sup> Studies have demonstrated that there is increased fibrosis in specimens removed from patients with AVF failure.<sup>3,41</sup> Masson's trichrome staining and pSMAD3 were performed to assess the fibrotic changes in outflow veins. There was reduction in trichrome and pSMAD3 staining in SV-treated vessels representing a decrease in vessel fibrosis compared with the control and MP groups, which is consistent with previous studies.<sup>42</sup> When SV was delivered to the periadventitia of the AVF outflow vein with chronic kidney disease, there was a significant decrease in the neointimal area and cell density together with an increase in the lumen vessel area/neointimal area ratio. Histological observations of the SV-treated vessels at day 28 after AVF creation demonstrated a significant decrease in α-SMA, FSP-1, and MYH11 positive cells.

MCP-1 has been shown to mediate TGF-β1 induced migration of vascular smooth muscle cells via SMAD3.<sup>43</sup> Inflammatory cells and macrophages can

**Figure 8. Immunohistochemistry staining for MCP-1 and CD68.**

There is decreased inflammation in SV-treated vessels compared with control and MP group as assessed by MCP-1 and CD68 staining. **A** and **B**, Representative sections of MCP-1 (**A**) and CD68 (**B**) staining at day 28. **C** and **D**, Semiquantitative analysis showed a significant decrease in the MCP-1 (C N=6, MP N=5, SV N=5) and the CD68-positive (C N=5, MP N=5, SV N=5) index in the SV-treated vessels compared with the control and MP group. Cells staining brown are positive for MCP-1 and CD68. Two-sample *t* test was performed (**C** and **D**). Each bar represents mean±SD. Significant differences are indicated by \**P*<0.05. Scale bar is 50 μm. C indicates controls; CD68, cluster of differentiation 68; MCP-1, monocyte chemoattractant protein-1; MP, microparticles; and SV, simvastatin.



regulate AVF patency and remodeling.<sup>44,45</sup> The adventitia and perivascular tissue surrounding the fistula play a major role in regulation of inflammation, cell recruitment, and cell proliferation after vascular injury.<sup>46,47</sup>

There are several studies showing that SV might modulate expression of MCP-1 and CD68.<sup>48,49</sup> Consistent with these studies, we observed that the gene expression of *Mcp-1* was decreased in SV-treated vessels at

day 3. Meanwhile, there was more MCP-1 and CD68 positive cells observed in the media and adventitia layers in the control and MP-treated vessels compared with statin-treated vessels at day 28.

In AVF failure, there is increased cell proliferation and decreased apoptosis. Previous study from our laboratory demonstrated that systemic delivery of SV resulted in a significant decrease in average Ki-67 staining with a significant increase in TUNEL staining. In the present study, SV-treated vessels had a significant decrease in proliferation with an increase in TUNEL staining.

Soluble cyclodextrin (CD) has been used for several decades to increase the solubility of hydrophobic drugs.<sup>50</sup> The cyclodextrin polymers used in this study harness the molecular inclusion complex formation between CD and soluble drugs to form an insoluble drug delivery depot capable of delivering SV for at least 14 days. Three different sizes of CD rings are widely available with additional modifications of ring hydroxyl groups that can be used to tailor the affinity of drug for the CD pocket to further adjust the localized delivery rate. Some burst release is still observed, which we believe is likely the result of a combination of 2 factors: (1) some unbound drug remains after loading and washing that immediately is available for release; and (2) fully loaded CDP at t=0 represents saturation of drug; CD pocket inclusion formation. A given molecule of SV that dissociates from a CD pocket and begins diffusing away is unlikely to interact with another free CD pocket before diffusion away from the CDP.<sup>51,52</sup> This case is even more likely at or near the surface of CDP particles. The thermodynamic favorability of drug-CD inclusion formation enables our CDPs to be refilled in situ after implantation,<sup>53</sup> which is important for preventing vascular access failure as the length of necessary treatment is an unresolved question. Thus, our CDPs are an ideal platform to provide sustained delivery of statin drugs to minimize VNH in AVFs.

There are several limitations to this study. First, the AVF was created using a cuff method, which may not mimic AVF creation in humans. However, some previous studies suggest that this procedure in mice could recapitulate AVF pathology.<sup>4,10,27</sup> Second, only 1 statin was tested in the current study, but the mechanisms of statins are similar.<sup>54</sup> Third, the CDPs had an effect on reducing gene expression of *Vegf-A* and *Mmp-9* in cell culture, which was not observed in vivo.

In summary, periadventitial delivery of controlled-release SV from CDP attenuates VNH for 4 weeks after AVF creation. This therapy offers a potential advantage to systemic therapy as there is directed drug delivery and potential reduction for potential problems with systemic delivery such as muscle pain and liver function abnormalities. Periadventitial delivery of CDP particles to the outflow vein at the time of AVF creation could be performed as was done in clinical trials using stem cell

delivery and vonapanitase.<sup>55,56</sup> These findings suggest that CDP coated statins have the therapeutic potential to reduce AVF failure and future studies in large animals need to be performed to validate these results before clinical trials are initiated.

## ARTICLE INFORMATION

Received July 7, 2020; accepted October 22, 2020.

### Affiliations

From the Vascular and Interventional Radiology Translational Laboratory, Department of Radiology, Mayo Clinic, Rochester, MN (C.Z., C.C., S.K., A.S., M.S., S.M.); Department of Vascular Surgery, The Second Xiangya Hospital, Central South University, Changsha, Hunan, China (C.Z.); Affinity Therapeutics, LLC, Cleveland, OH (S.T.Z., J.N.K.); Department of Vascular Surgery, Union Hospital, Tongji Medical College, Huazhong University of Science and Technology, Wuhan, China (C.C.); Department of Biomedical Engineering, Case Western Reserve University, Cleveland, OH (H.A.v.R.); and Department of Biochemistry and Molecular Biology, Mayo Clinic, Rochester, MN (S.M.).

### Acknowledgments

We acknowledge the assistance of Lucy Bahn, PhD, in preparation of this article.

Author contributions: Zhao and Misra designed research; Zhao, Cai, and Misra analyzed data; Zhao, Zuckerman, Cai, Kilari, Singh, Simeon, Korley, von Recum, and Misra performed research; Zhao, Zuckerman, and Misra wrote the paper.

### Sources of Funding

This work was funded by National Institutes of Health (NIH) grants HL137549 (Zuckerman), HL098967 (Misra), and DK107870 (Misra). This work is the property of Affinity Therapeutics LLC and was funded by NIH Small Business Innovation Research (SBIR) grant 5R43HL137549.

### Disclosures

None.

## REFERENCES

- Riella MC, Roy-Chaudhury P. Vascular access in haemodialysis: strengthening the Achilles' heel. *Nat Rev Nephrol*. 2013;9:348.
- Brescia MJ, Cimino JE, Appel K, Hurwicz BJ. Chronic hemodialysis using venipuncture and a surgically created arteriovenous fistula. *N Engl J Med*. 1966;275:1089-1092.
- Al-Jaishi AA, Oliver MJ, Thomas SM, Lok CE, Zhang JC, Garg AX, Kosa SD, Quinn RR, Moist LM. Patency rates of the arteriovenous fistula for hemodialysis: a systematic review and meta-analysis. *Am J Kidney Dis*. 2014;63:464-478.
- Misra S, Shergill U, Yang B, Janardhanan R, Misra KD. Increased expression of HIF-1 $\alpha$ , VEGF-A and its receptors, MMP-2, TIMP-1, and ADAMTS-1 at the venous stenosis of arteriovenous fistula in a mouse model with renal insufficiency. *J Vasc Interv Radiol*. 2010;21:1255-1261.
- Juncos JP, Grande JP, Kang L, Ackerman AW, Croatt AJ, Katusic ZS, Nath KA. MCP-1 contributes to arteriovenous fistula failure. *J Am Soc Nephrol*. 2011;22:43-48.
- Wong C, Bezhaeva T, Rothuizen TC, Metselaer JM, de Vries MR, Verbeek FPR, Vahrmeijer AL, Wezel A, van Zonneveld A-J, Rabelink TJ, et al. Liposomal prednisolone inhibits vascular inflammation and enhances venous outward remodeling in a murine arteriovenous fistula model. *Sci Rep*. 2016;6:1-10.
- Misra S, Fu AA, Rajan DK, Juncos LA, McKusick MA, Bjarnason H, Mukhopadhyay D. Expression of hypoxia inducible factor-1 $\alpha$ , macrophage migration inhibition factor, matrix metalloproteinase-2 and-9, and their inhibitors in hemodialysis grafts and arteriovenous fistulas. *J Vasc Interv Radiol*. 2008;19:252-259.
- Goldstein JL, Brown MS. A century of cholesterol and coronaries: from plaques to genes to statins. *Cell*. 2015;161:161-172.

9. Lefer DJ. Statins as Potent Antiinflammatory Drugs. *Circulation*. 2002;106:2041–2042.
10. Janardhanan R, Yang B, Vohra P, Roy B, Withers S, Bhattacharya S, Mandrekar J, Kong H, Leaf EB, Mukhopadhyay D, et al. Simvastatin reduces venous stenosis formation in a murine hemodialysis vascular access model. *Kidney Int*. 2013;84:338–352.
11. Zhang L, Lu H, Huang J, Guan Y, Sun H. Simvastatin exerts favourable effects on neointimal formation in a mouse model of vein graft. *Eur J Vasc Endovasc Surg*. 2011;42:393–399.
12. Qiang B, Toma J, Fujii H, Oshero AB, Nili N, Sparkes JD, Fefer P, Samuel M, Butany J, Leong-Poi H, et al. Statin therapy prevents expansive remodeling in venous bypass grafts. *Atherosclerosis*. 2012;223:106–113.
13. Zhang L, Jin H, Huang J, Lu H, Guan Y, Chen X, Sun H. Local delivery of pravastatin inhibits intimal formation in a mouse vein graft model. *Can J Cardiol*. 2012;28:750–757.
14. Cui J, Kessinger CW, Jhaji HS, Grau MS, Misra S, Libby P, McCarthy JR, Jaffer FA. Atorvastatin reduces in vivo fibrin deposition and macrophage accumulation, and improves primary patency duration and maturation of murine arteriovenous fistula. *J Am Soc Nephrol*. 2020;31:931–945.
15. Chang H-H, Chang Y-K, Lu C-W, Huang C-T, Chien C-T, Hung K-Y, Huang K-C, Hsu C-C. Statins improve long term patency of arteriovenous fistula for hemodialysis. *Sci Rep*. 2016;6:1–10.
16. Martinez L, Duque JC, Escobar LA, Tabbara M, Asif A, Fayad F, Vazquez-Padron RI, Salman LH. Distinct impact of three different statins on arteriovenous fistula outcomes: a retrospective analysis. *J Vasc Access*. 2016;17:471–476.
17. Kuji T, Masaki T, Goteti K, Li L, Zhuplatov S, Terry CM, Zhu W, Leyboldt JK, Rathi R, Blumenthal DK, et al. Efficacy of local dipyridamole therapy in a porcine model of arteriovenous graft stenosis. *Kidney Int*. 2006;69:2179–2185.
18. Rajathurai T, Rizvi SI, Lin H, Angelini GD, Newby AC, Murphy GJ. Periadventitial rapamycin-eluting microbeads promote vein graft disease in long-term pig vein-into-artery interposition grafts. *Circ Cardiovasc Interv*. 2010;3:157–165.
19. Sanders WG, Hogrebe PC, Grainger DW, Cheung AK, Terry CM. A biodegradable perivascular wrap for controlled, local and directed drug delivery. *J Control Release*. 2012;161:81–89.
20. Yu X, Takayama T, Goel SA, Shi X, Zhou Y, Kent KC, Murphy WL, Guo L-W. A rapamycin-releasing perivascular polymeric sheath produces highly effective inhibition of intimal hyperplasia. *J Control Release*. 2014;191:47–53.
21. Menei P, Benoit J-P. Implantable drug-releasing biodegradable microspheres for local treatment of brain glioma. In: Westphal M, Tonn JC, Ram Z, eds. *Local Therapies for Glioma Present Status and Future Developments*. *Acta Neurochirurgica Supplements*. Vol. 88. Vienna: Springer; 2003. [https://doi.org/10.1007/978-3-7091-6090-9\\_9](https://doi.org/10.1007/978-3-7091-6090-9_9).
22. Sy JC, Seshadri G, Yang SC, Brown M, Oh T, Dikalov S, Murthy N, Davis ME. Sustained release of a p38 inhibitor from non-inflammatory microspheres inhibits cardiac dysfunction. *Nat Mater*. 2008;7:863–868.
23. Haley RM, Zuckerman ST, Gormley CA, Korley JN, von Recum HA. Local delivery polymer provides sustained antifungal activity of amphotericin B with reduced cytotoxicity. *Exp Biol Med (Maywood)*. 2019;244:526–533.
24. Grafmiller KT, Zuckerman ST, Petro C, Liu L, von Recum HA, Rosen MJ, Korley JN. Antibiotic-releasing microspheres prevent mesh infection in vivo. *J Surg Res*. 2016;206:41–47.
25. Misra S, Fu AA, Misra KD, Shergill UM, Leaf EB, Mukhopadhyay D. Hypoxia-induced phenotypic switch of fibroblasts to myofibroblasts through a matrix metalloproteinase 2/tissue inhibitor of metalloproteinase-mediated pathway: implications for venous neointimal hyperplasia in hemodialysis access. *J Vasc Interv Radiol*. 2010;21:896–902.
26. Kilari S, Yang B, Sharma A, McCall DL, Misra S. Increased transforming growth factor beta (TGF- $\beta$ ) and pSMAD3 signaling in a murine model for contrast induced kidney injury. *Sci Rep*. 2018;8:1–12.
27. Kilari S, Cai C, Zhao C, Sharma A, Chernogubova E, Simeon M, Wu CC, Song HL, Maegdefessel L, Misra S. The role of microRNA-21 in venous neointimal hyperplasia: implications for targeting miR-21 for VNH treatment. *Mol Ther*. 2019;27:1681–1693.
28. Cai C, Kilari S, Singh AK, Zhao C, Simeon ML, Misra A, Li Y, Misra S. Differences in transforming growth factor-beta1/BMP7 signaling and venous fibrosis contribute to female sex differences in arteriovenous fistulas. *J Am Heart Assoc*. 2020;9:e017420. DOI: 10.1161/JAHA.120.017420.
29. Cai C, Kilari S, Zhao C, Simeon ML, Misra A, Li Y, van Wijnen AJ, Mukhopadhyay D, Misra S. Therapeutic effect of adipose derived mesenchymal stem cell transplantation in reducing restenosis in a murine angioplasty model. *J Am Soc Nephrol*. 2020;31:1781–1795.
30. Cai C, Yang B, Kilari S, Li Y, Zhao C, Sharma A, Misra S. Evaluation of venous stenosis angioplasty in a murine arteriovenous fistula model. *J Vasc Interv Radiol*. 2019;30:1512–1521.e1513.
31. Cai C, Zhao C, Kilari S, Sharma A, Singh AK, Simeon ML, Misra A, Li Y, Misra S. Effect of sex differences in treatment response to angioplasty in a murine arteriovenous fistula model. *Am J Physiol Renal Physiol*. 2020;318:F565–F575.
32. Janardhanan R, Yang B, Kilari S, Leaf EB, Mukhopadhyay D, Misra S. The role of repeat administration of adventitial delivery of lentivirus-shRNA-Vegf-A in arteriovenous fistula to prevent venous stenosis formation. *J Vasc Interv Radiol*. 2016;27:576–583.
33. Brahmabhatt A, NievesTorres E, Yang B, Edwards WD, Chaudhury PR, Lee MK, Kong H, Mukhopadhyay D, Kumar R, Misra S. The role of iex-1 in the pathogenesis of venous neointimal hyperplasia associated with hemodialysis arteriovenous fistula. *PLoS One*. 2014;9:e102542.
34. Riessen R, Axel D, Fenchel M, Herzog U, Rossmann H, Karsch K. Effect of HMG-CoA reductase inhibitors on extracellular matrix expression in human vascular smooth muscle cells. *Basic Res Cardiol*. 1999;94:322–332.
35. Stracke S, Konner K, Kostlin I, Friedl R, Jehle PM, Hombach V, Keller F, Waltenberger J. Increased expression of TGF-beta1 and IGF-I in inflammatory stenotic lesions of hemodialysis fistulas. *Kidney Int*. 2002;61:1011–1019.
36. Zegarska J, Paczek L, Pawlowska M, Wyczalkowska A, Michalska W, Ziolkowski J, Gorski A, Rowinski W, Kosieradzki M, Kwiatkowski A, et al. Increased mRNA expression of transforming growth factor beta in the arterial wall of chronically rejected renal allografts in humans. *Transplant Proc*. 2006;38:115–118.
37. Brahmabhatt A, Misra S. The biology of hemodialysis vascular access failure. *Semin Intervent Radiol*. 2016;33:015–020.
38. Misra S, Fu AA, Puggioni A, Glockner JF, Rajan DK, McKusick MA, Bjarnason H, Mukhopadhyay D. Increased expression of hypoxia-inducible factor-1 $\alpha$  in venous stenosis of arteriovenous polytetrafluoroethylene grafts in a chronic renal insufficiency porcine model. *J Vasc Interv Radiol*. 2008;19:260–265.
39. Yang B, Janardhanan R, Vohra P, Greene EL, Bhattacharya S, Withers S, Roy B, Nieves Torres EC, Mandrekar J, Leaf EB, et al. Adventitial transduction of lentivirus-shRNA-VEGF-A in arteriovenous fistula reduces venous stenosis formation. *Kidney Int*. 2014;85:289–306.
40. Ruiz-Ortega M, Rodríguez-Vita J, Sanchez-Lopez E, Carvajal G, Egido J. TGF- $\beta$  signaling in vascular fibrosis. *Cardiovasc Res*. 2007;74:196–206.
41. Martinez L, Duque JC, Tabbara M, Paez A, Selman G, Hernandez DR, Sundberg CA, Tey JCS, Shiu Y-T, Cheung AK, et al. Fibrotic venous remodeling and nonmaturation of arteriovenous fistulas. *J Am Soc Nephrol*. 2018;29:1030–1040.
42. Yang T, Chen M, Sun T. Simvastatin attenuates TGF- $\beta$ 1-induced epithelial-mesenchymal transition in human alveolar epithelial cells. *Cell Physiol Biochem*. 2013;31:863–874.
43. Ma J, Wang Q, Fei T, Han J-DJ, Chen Y-G. MCP-1 mediates TGF- $\beta$ -induced angiogenesis by stimulating vascular smooth muscle cell migration. *Blood*. 2007;109:987–994.
44. Bush HL Jr, Jakubowski JA, Curl GR, Deykin D, Nabseth DC. The natural history of endothelial structure and function in arterialized vein grafts. *J Vasc Surg*. 1986;3:204–215.
45. Kwei S, Stavrakis G, Takahas M, Taylor G, Folkman MJ, Gimbrone MA Jr, García-Cardeña G. Early adaptive responses of the vascular wall during venous arterialization in mice. *Am J Pathol*. 2004;164:81–89.
46. Miller FJ Jr. Adventitial fibroblasts: backstage journeymen. *Arterioscler Thromb Vasc Biol*. 2001;21:722–723.
47. Michel J-B, Thauant O, Houard X, Meilhac O, Caligiuri G, Nicoletti A. Topological determinants and consequences of adventitial responses to arterial wall injury. *Arterioscler Thromb Vasc Biol*. 2007;27:1259–1268.
48. Tuomisto TT, Lumivuori H, Kansanen E, Häkkinen S-K, Turunen MP, Van Thienen JV, Horrevoets AJ, Levonen A-L, Ylä-Herttuala S. Simvastatin has an anti-inflammatory effect on macrophages via upregulation of an atheroprotective transcription factor, Kruppel-like factor 2. *Cardiovasc Res*. 2008;78:175–184.
49. Feig JE, Shang Y, Rotllan N, Vengrenyuk Y, Wu C, Shamir R, Torra IP, Fernandez-Hernando C, Fisher EA, Garabedian MJ. Statins promote the regression of atherosclerosis via activation of the CCR7-dependent emigration pathway in macrophages. *PLoS One*. 2011;6:e28534.

- 
50. Davis ME, Brewster ME. Cyclodextrin-based pharmaceuticals: past, present and future. *Nat Rev Drug Discov.* 2004;3:1023–1035.
  51. Vulic K, Shoichet MS. Affinity-based drug delivery systems for tissue repair and regeneration. *Biomacromol.* 2014;15:3867–3880.
  52. Zuckerman ST, Rivera-Delgado E, Haley RM, Korley JN, von Recum HA. Elucidating the structure-function relationship of solvent and cross-linker on affinity-based release from cyclodextrin hydrogels. *Gels.* 2020;6:9.
  53. Cyphert EL, Zuckerman ST, Korley JN, von Recum HA. Affinity interactions drive post-implantation drug filling, even in the presence of bacterial biofilm. *Acta Biomater.* 2017;57:95–102.
  54. Kessinger CW, Kim JW, Henke PK, Thompson B, McCarthy JR, Hara T, Sillesen M, Margey RJP, Libby P, Weissleder R, et al. Statins improve the resolution of established murine venous thrombosis: reductions in thrombus burden and vein wall scarring. *PLoS One.* 2015;10:e0116621.
  55. Conte MS, Nugent HM, Gaccione P, Roy-Chaudhury P, Lawson JH. Influence of diabetes and perivascular allogeneic endothelial cell implants on arteriovenous fistula remodeling. *J Vasc Surg.* 2011;54:1383–1389.
  56. Peden EK, O'Connor TP, Browne BJ, Dixon BS, Schanzer AS, Jensik SC, Sam AD II, Burke SK. Arteriovenous fistula patency in the 3 years following vonapanitase and placebo treatment. *J Vasc Surg.* 2017;65:1113–1120.